



## INFLAMMATION-RELATED OXIDATIVE STRESS IN WHITE ADIPOSE TISSUES OF AN INBRED OBESE PIG\*

X.F. Yang, Z.Y. Jiang\*, Z.M. Tian, Y.Q. Qiu, L. Wang, K.G. Gao, Y.J. Hu, X.Y. Ma

Laboratory of Animal Nutrition and Feed (South China), Ministry of Agriculture; State Key Laboratory of Livestock and Poultry Breeding; Guangdong Public Laboratory of Animal Breeding and Nutrition; Institute of Animal Science, Guangdong Academy of Agricultural Sciences, Guangzhou, 510640, P. R. China

\*Corresponding author: jiangz28@qq.com

### Abstract

The uneven development of adipose tissues reflects a differential occurrence of biological events *in vivo* while the underlying molecular mechanism remains largely unknown. In the present study, the *in vivo* inflammatory status of an inbred obese porcine model, Lantang pig, was assessed, aiming to provide evidence for obesity biology. Compared with genetically lean pigs (crossbred, Duroc × Landrace × Large White), Lantang pigs exhibited a larger amount of ultra large adipocytes in subcutaneous adipose tissue accompanied with higher expression of macrophage/monocytes markers and pro-inflammatory genes (TLR4, CD14, CD11 $\beta$ , MCP1, TNF $\alpha$ , IL1 $\beta$  and IL6) and lower expression of cellular antioxidant enzymes (SOD1, 2 and 3). Plasma concentrations of LPS and TNF- $\alpha$  were also higher in Lantang pigs than in lean pigs. Among adipose tissues of Lantang pigs, the subcutaneous tissue had the most abundant expression of inflammation related genes (TLR4, CD14, TNF $\alpha$  and IL6) and the lowest level of cellular antioxidant genes (SOD 1 and 2), while the perirenal adipose tissue had opposite profile. Significant activation of p38 MAPK pathway was indicated by increased phosphorylation of p38 in the subcutaneous adipose tissue of Lantang pigs. Collectively, the bacteria-derived LPS induced inflammation-associated oxidative stress indeed exists in adipose tissues of Lantang pig, and the differential expressions of inflammatory and antioxidant genes, to some extent, account for the uneven development of the adipose tissue within bodies.

**Key words:** obese pig, adipose tissue, oxidative stress, LPS, inflammation

Obesity has become a global epidemic and stimulates tremendous efforts in prevention and intervention (Bray and Bellanger, 2006; Wisse et al., 2007). Much progress has been made on defining the molecular mechanism of obesity and related dis-

---

\*Work financed from: National Basic Research Program of China (2013CB127301 and 2013CB127304). China Agriculture Research System (CARS-36). Presidential Foundation of Guangdong Academy of Agricultural Sciences (201312).

orders in humans with the help of mouse and rat models. However, the discrepancy in adipose tissue biology between humans and rodent somewhat hinders the research progress and effective transition of existing knowledge to an alleviation of human obesity. With higher physiological similarities to human than the frequently used rodent models, pigs are recognized as a better model for obesity biology (Spurlock and Gabler, 2008). Here we reported the molecular characteristics of white adipose tissue in an inbred obese pig model, Lantang pig, aiming to facilitate the understanding of adiposity development.

Obesity is characterized by excess development of adipose tissues, especially the subcutaneous and omental adipose tissues (Wajchenberg, 2000). Several studies have demonstrated that in obesity masses of regional adipose tissues were differentially correlated with important metabolic syndrome, including abnormal plasma glucose, insulin, and lipid concentrations (Kim et al., 2011; Wajchenberg, 2000). The pattern of adipokines secretion and the sensitivity to hormones were also significantly different among adipose tissues (Arner, 1995; Motoshima et al., 2002). Hotamisligil et al. first found a pro-inflammatory factor, tumor necrosis factor (TNF)- $\alpha$ , was highly correlated to adipose accumulation (Hotamisligil et al., 1993). Since then, chronic inflammation in adipose tissues was further reported to be associated with macrophage infiltration, and increased secretion of pro-inflammatory cytokines such as monocyte chemoattractant MCP-1, TNF- $\alpha$ , interleukin (IL)-1 $\beta$ , and IL-6 in rodent models (Deng et al., 2013; Hotamisligil et al., 1993; Tilg and Moschen, 2006; Weisberg et al., 2003). The major causative factor of inflammation in adipose tissue was referred to a bacteria-derived metabolite, lipopolysaccharide (LPS) (Caesar et al., 2012). Expression of Toll-like Receptors (TLRs) and pro-inflammatory genes in different adipose tissues responded differently to diet-induced and genetic obesity in mice (Kim et al., 2012), indicating an important role of innate immunity in adiposity regulation. However, the detailed characteristics of inflammatory processes in different adipose tissues remain to be identified in order to elucidate the uneven development of adiposity.

Reactive oxygen species (ROS), derived from respiration or other cellular processes, are potential pro-inflammatory factors (Di et al., 2012). Under healthy conditions, cellular antioxidant system is able to remove ROS instantly and maintain a stable redox environment. However, in adipose tissues of obese human and mice, the expression of major antioxidant enzymes such as copper, zinc superoxide dismutase (SOD) and glutathione peroxidase is compromised (Di Renzo et al., 2010; Furukawa et al., 2004; Kanda et al., 2011). It has been shown that ROS induced pro-inflammatory response in cells or mice by regulating NF- $\kappa$ B (Yeop et al., 2010) and/or p38 MAPK (Park et al., 2015; Youn et al., 2016) pathways. Treatment with antioxidant agents alleviated inflammation in adipose tissue of mice fed high fat diet (Pires et al., 2013). However, the role of antioxidant enzymes in adiposity development is not fully understood. A comparison of gene expressions of antioxidant enzymes among tissues would facilitate the understanding of their functions in adiposity/obesity development.

In the present study, obese Lantang pigs were applied for the first time to study the obesity development, aiming to provide evidence for obesity biology. We found

an existence of stronger inflammation-associated oxidative stress in subcutaneous adipose tissue in the obese model, which, to some extent, resulted from the over-secretion of LPS and suppressed expression of antioxidant enzymes.

## Material and methods

### Animals and treatments

Animal care and experimental procedures were approved by Animal Experimental Committee of the Institute of Animal Science, Guangdong Academy of Agricultural Sciences. Conventional Lean pigs (Duroc  $\times$  Landrace  $\times$  Large White, DLW) and inbred obese pigs (Lantang, Chinese local inbred strain) were studied. Twenty pigs (15–20 kg, male, castrated on birth) per genotype were given free access to a corn-soybean meal-based diet for 16 weeks. At the end of experiment, pigs were food deprived for 12 h and blood from the posterior auricular vein was collected to obtain plasma. Seven pigs out of the 20 pigs were randomly selected and euthanized by exsanguination after electronarcosis. Carcass was split longitudinally through the vertebrae midline and the left side was kept. Samples of dorsal subcutaneous adipose tissue (SC) located above the 10th rib, of omental adipose tissue (OM) and of perirenal adipose tissue (PR) were collected and snap-frozen in liquid nitrogen immediately after euthanization.

### Morphological examination

Frozen adipose tissue sections (10  $\mu\text{m}$ ) were cut in the cryostat chamber at  $-18^{\circ}\text{C}$  to  $-20^{\circ}\text{C}$  followed by H&E staining. For each individual adipose depot, at least four different high-power fields from each section were examined at 50X magnification using a Zeiss Axio Scope A1 microscope (Carl Zeiss Inc., Göttingen, Germany). Adipocyte cross-sectional area was determined for each adipocyte in each field analyzed using ImageJ software with adipocyte size plugin (<http://rsb.info.nih.gov/ij/>) and the actual size in  $\mu\text{m}^2$  of adipocytes was adjusted according to the magnification factor (1:2500). Values less than 500  $\mu\text{m}^2$  were assumed to represent artifacts from the image-conversion process and were excluded from analysis. Average distribution of adipocyte cross-sectional area was calculated from the seven representative animals of each genotype using Microsoft Excel (Microsoft Corp., Redmond, Washington, USA).

### RNA extraction and Real-time PCR

Total RNA was extracted using Trizol (Life Technologies, Inc., Grand Island, NY, USA) kit following the manufacturer's instructions. Total RNA (10  $\mu\text{g}$ ) was reverse transcribed and quantitative real-time PCR was performed using the SYBR Green method with 7900HT Fast Real-Time PCR System (Life Technologies). Primer sequences used are listed in Table 1. Fold changes of mRNA abundance for genes of interest were calculated using the  $2^{-\Delta\Delta\text{CT}}$  method (Livak and Schmittgen, 2001). Amplification of Glyceraldehyde 3-phosphate dehydrogenase (GAPDH) from each sample was used for normalizing quantitative PCR data.

Table 1. Primer sequences for targeted genes

Gene	Primer sequence
TLR4	F: 5' TGACGCCTTTGTTATCTACTCC 3' R: 5' GGTCCTGGGCAATCTCATACTC 3'
TNF $\alpha$	F: 5' AATTTGCAGGCTGTTTCTGC 3' R: 5' TATGAAGGTGGTGCAGATGG 3'
IL-1 $\beta$	F: 5' CTCAGCCAGTCTTCATTGTTCC 3' R: 5' TGCCTGATGCTCTTGTTC 3'
IL-6	F: 5' CGCCTTCAGTCCAGTCGC 3' R: 5' GGCATCACCTTTGGCATCT 3'
CAT1	F: 5' CATCAAAAAGTGGCAGTCA 3' R: 5' TGGTAGCGATGCAGTCAAAG 3'
CD14	F: 5' CCTGGACCTATCTGACAATC 3' R: 5' GAGATCAAGCACGGTGAG 3'
CD11 $\beta$	F: 5' AGAACATAACACGCAGACA 3' R: 5' CGATAGGACAAGCCAGAC 3'
MCP1	F: 5' CAGCAGCAAGTGTCTAA 3' R: 5' CAGGTGGCTTATGGAGTC 3'
GAPDH	F: 5' CTTATTGACCTCCACTACA 3' R: 5' CATTGCTGACGATCTTGAG 3'
SOD1	F: 5' GAGAAGACAGTGTAGTAACG 3' R: 5' CTCTGCCCAAGTCATCTG 3'
SOD2	F: 5' CGTCGTGGAGGAGAAGTA 3' R: 5' GTAGAACAAGCGGCAATC 3'
SOD3	F: 5' CTGTGCTTACCTGCTCCT 3' R: 5' CGAAGTTGCCGAAGTCTC 3'
GPX1	F: 5' CCTCAAGTACGTCCGACCAG 3' R: 5' TTCCATGCGATGCATTGCG 3'

### Measurements of plasma LPS and TNF- $\alpha$

Plasma LPS concentration was determined using the Toxin Sensor Chromogenic LAL Endotoxin Assay Kit (GenScript, Piscataway, NJ, USA). All plasma samples were extracted with chloroform prior to the LAL assay as described by Harris et al. (1990). Briefly, the diluted plasma was mixed in a ratio of 1:1 (v/v) with chloroform and incubated for 1 hour in a thermostat block (25°C) with shaking at 800 rpm. Then the emulsion was separated by centrifugation at 2,000 g for 20 min and the top aqueous layer was collected for endotoxin assay. The appropriate dilution factors were determined previously to make sure the measurements fall in the range of the standard curve. Measurements of TNF- $\alpha$  concentration in plasma were performed using porcine TNF- $\alpha$  Elisa kit (Thermo Scientific Pierce, Rockford, IL, USA) according to the manufacturer's instructions.

### Western blot

Adipose tissues were homogenized on ice in RIPA lysis buffer (50 mM Tris-HCl, pH 7.4, 150 mM NaCl, 1% Triton X-100, 0.1% sodium dodecyl sulfate, 0.5% deoxycholic acid, 5  $\mu$ g/ml aprotinin, 10  $\mu$ g/ml leupeptin, 1  $\mu$ M PMSF, 1 mM sodium fluoride) and centrifuged at 10,000 g for 10 min at 4 degree to collect protein extracts. The protein concentration was measured by using BCA Protein Assay Kit (Pierce Biotechnology, Rockford, IL, USA). Typically, 20–40  $\mu$ g protein was resolved by

electrophoresis on 10% SDS-polyacrylamide gel and electrophoretically transferred to PVDF or nitrocellulose membrane. The membranes were blocked with 5% nonfat dry milk and probed overnight with rabbit anti-TLR4 (Santa Cruz Biotechnology Inc., Santa Cruz, California, USA), or mouse anti-P38 and anti-phosphorylated P38 antibodies (Cell Signaling Technology Inc., Beverly, Massachusetts, USA). Detection of specific bands was carried out by Super Signal chemiluminescent substrate (Pierce Biotechnology) visualized on a Molecular Imager ChemiDoc XRS system using Quantity One software (Bio-Rad, Hercules, CA, USA).

### Data analysis and statistics

Data are expressed as means  $\pm$  SEM. The statistical significance between two genotypes was evaluated by Student's *t* test, the significance between tissues was assessed by one-way ANOVA, followed by post-hoc Duncan test for multiple comparisons. A P-value less than 0.05 was considered to indicate a significant difference.

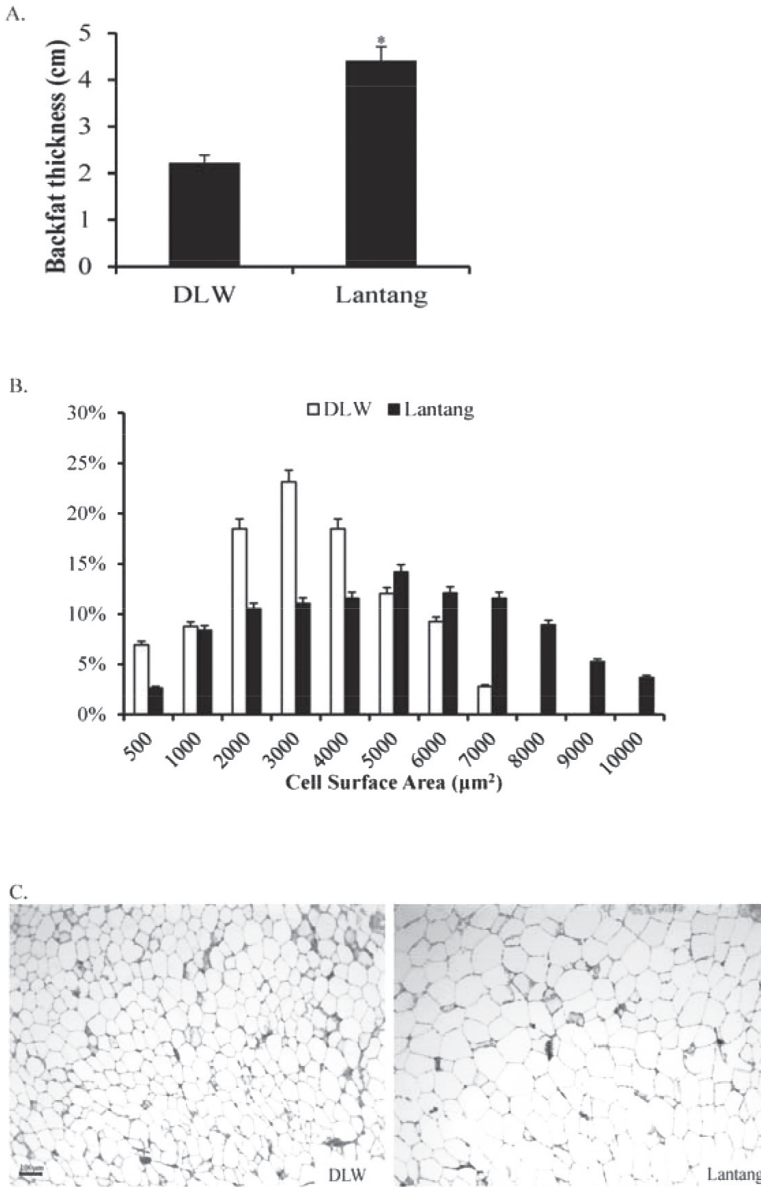
## Results

### Development of subcutaneous adipose tissue in Lantang pigs

Compared with DLW, Lantang pigs had much more subcutaneous fat deposit. The thickness of dorsal SC above 10th rib was over two-fold that in DLW ( $P < 0.01$ , Figure 1 A). Fat deposits in other organs or locations, such as omental and perirenal position, were also remarkably abundant in Lantang pigs (unpublished data). As indicated by the morphological analysis, Lantang pigs had some ultra large adipocytes and higher frequency for large adipocytes' appearance in SC (Figure 1 B and C). The most abundant adipocytes (high frequency) were about  $3000 \mu\text{m}^2$  and  $5000 \mu\text{m}^2$  in size for DLW and Lantang pigs, respectively.

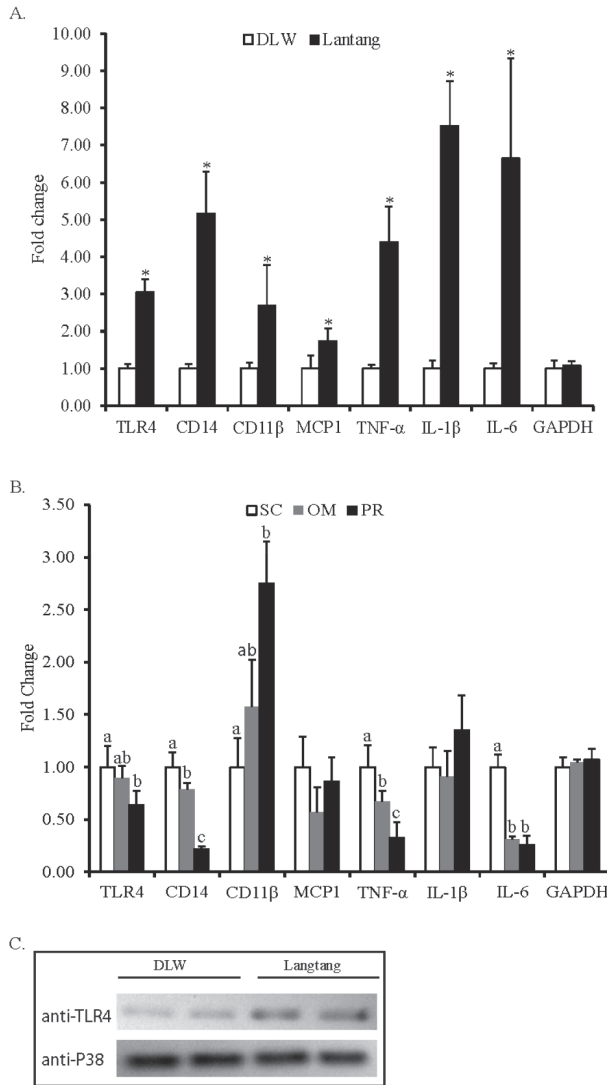
### The mRNA expression of inflammatory genes in white adipose tissues

To explore the inflammatory status, expressions of interleukin and cell surface marker genes in white adipose tissues were measured. As shown in Figure 2 A, mRNA levels of MCP-1, TNF- $\alpha$ , IL-1 $\beta$  and IL-6 genes in SC were significantly higher in Lantang than in DLW pigs ( $P < 0.001$ ). Similarly, mRNA abundance of cell surface markers, TLR4, CD14 and CD11 $\beta$ , was also significantly higher in Lantang than in DLW pigs ( $P < 0.05$ ). Results of Western blot further confirmed that expression of TLR4 in subcutaneous adipose tissue was higher in Lantang than in DLW pigs (Figure 2 C). To assess the difference in inflammatory status among adipose tissues in Lantang pig, gene expression of pro-inflammatory markers in subcutaneous, omental and perirenal adipose tissues was measured. As shown in Figure 2 B, compared with perirenal adipose, subcutaneous adipose tissue had higher mRNA levels of TLR4, CD14, TNF- $\alpha$ , and IL-6 ( $P < 0.05$ ), and lower expression of CD11 $\beta$  ( $P < 0.05$ ). Abundance of TLR4, CD14, CD11 $\beta$ , TNF- $\alpha$ , and IL-6 mRNAs in omental adipose tissue were in the middle among those levels of SC and PR tissues. There was no statistical difference in MCP1 or IL-1 $\beta$  mRNA abundance among these tissues.



\* – values between DLW and Lantang pigs differ significantly ( $P < 0.05$ ).

Figure 1. Morphological analysis of subcutaneous adipose tissues. A) Thickness of dorsal subcutaneous adipose tissues of DLW and Lantang pigs (both  $n = 7$ ). B) Frequency distribution of adipocyte cell surface area. C) Representative images of dorsal subcutaneous adipose tissues with H&E staining

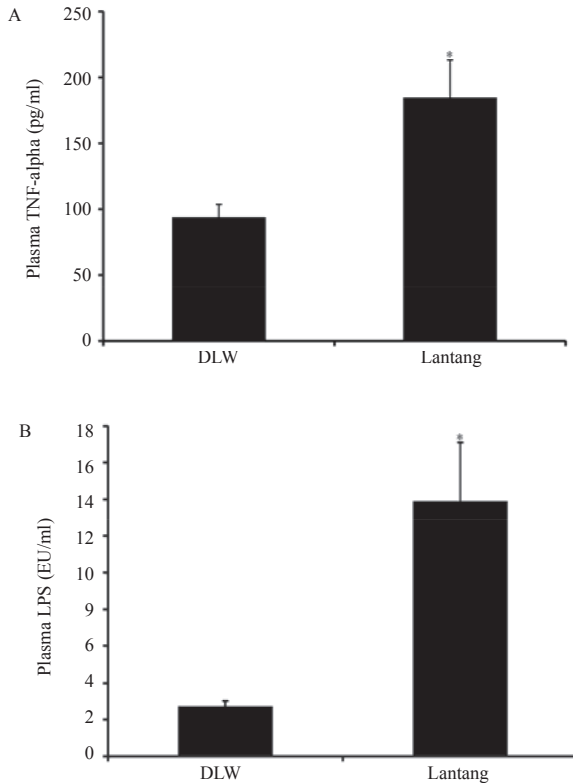


\* – values between DLW and Lantang pigs differ significantly ( $P < 0.05$ ); a, b, c – values in bars with different letters differ significantly ( $P < 0.05$ ).

Figure 2. Expression of inflammation related genes and proteins in adipose tissues. A) Real-time PCR analysis of Toll like receptor (TLR) 4, cluster designation (CD)14, CD11 $\beta$ , Monocyte chemoattractant protein (MCP) 1, Tumor necrosis factors  $\alpha$  (TNF- $\alpha$ ), Interleukin-1 $\beta$  (IL-1 $\beta$ ), IL-6 and Glyceraldehyde 3-phosphate dehydrogenase (GAPDH) mRNAs in subcutaneous adipose tissues of DLW and Lantang pigs (both  $n = 7$ ). B) Real-time PCR analysis of indicated genes in subcutaneous, omental and perirenal adipose in Lantang pigs ( $n = 7$ ). C) Western blot analysis of TLR4 in subcutaneous adipose tissues of DLW and Lantang pigs (both  $n = 7$ ). For each pig breed, 20  $\mu$ g of pooled protein samples was loaded to each well on the gel in total volume of 20  $\mu$ L (in loading buffer). SC, subcutaneous adipose tissue. OM, omental adipose tissue. PR, perirenal adipose tissue

### Endotoxemia with high level of plasma TNF- $\alpha$ in Lantang pig

As indicated in Figure 3, concentration of plasma LPS in Lantang pigs was about five fold that in DLW pigs ( $P < 0.001$ ). Similarly, blood TNF- $\alpha$  concentration in Lantang pigs was about two fold ( $184.39 \pm 28.88$  vs  $93.27 \pm 10.50$  pg/ml) that in DLW pigs ( $P < 0.001$ ), indicating that Lantang pigs had a higher level of chronic systematic inflammation.



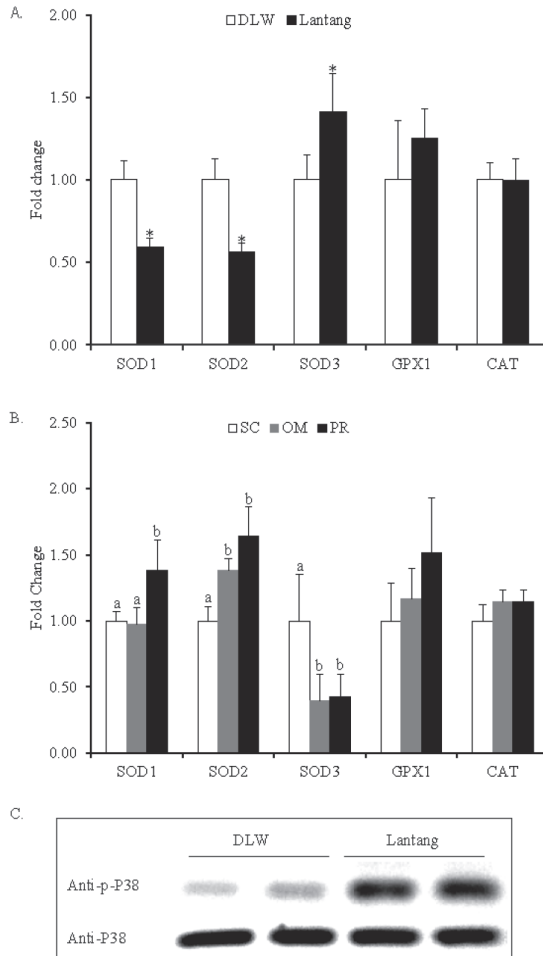
\* – values between DLW and Lantang pigs differ significantly ( $P < 0.05$ ).

Figure 3. Plasma concentrations of TNF- $\alpha$  (A) and LPS (B) in DLW and Lantang pigs (both  $n = 20$ )

### The mRNA expression of cellular antioxidant enzymes in subcutaneous adipose tissue with activated MAPK pathway in Lantang pigs

Levels of SOD1 and SOD2 mRNAs were significantly lower in subcutaneous adipose tissues of Lantang than those in DLW, while expression of the extracellular superoxide dismutase, SOD3, was up-regulated in Lantang pigs (all  $P < 0.05$ , Figure 4 A). In Lantang pigs, subcutaneous adipose tissue had less SOD1 and SOD2 mRNAs, but more SOD3 mRNA than perirenal adipose (all  $P < 0.05$ , Figure 4 B). There was no statistical difference in GPX1 or CAT mRNA levels either between two genotypes or among tissues. Additionally, the oxidative stress related activation of MAPK path-

way was measured. Results of Western blot indicated phosphorylated P38 in subcutaneous adipose were up-regulated in Lantang compared to DLW pigs (Figure 4 C). The phosphorylated JNK were hardly detected under this condition (data not shown).



\* – values between DLW and Lantang pigs differ significantly ( $P < 0.05$ ); a, b, c – values in bars with different letters differ significantly ( $P < 0.05$ ).

Figure 4. Gene expression of antioxidant enzymes and phosphorylation of MAPK P38 in adipose tissues. A) Real-time PCR analysis of copper, zinc superoxide (SOD1), MnSOD (SOD2), extracellular SOD (SOD3), glutathionine peroxidase (GPX1) and catalase (CAT) in subcutaneous adipose tissues of DLW and Lantang pigs (both  $n = 7$ ). B) Real-time PCR analysis of antioxidant genes indicated above in subcutaneous, omental and perirenal adipose in Lantang pigs ( $n = 7$ ). C) Western blot analysis of total and phosphorylated P38 proteins in adipose tissues of DLW and Lantang pigs (both  $n = 7$ ). For each pig breed, 20  $\mu\text{g}$  of pooled protein samples was loaded to each well on the gel in total volume of 20  $\mu\text{L}$  (in loading buffer). SC, subcutaneous adipose tissue. OM, omental adipose tissue. PR, perirenal adipose tissue

## Discussion

We report here for the first time that chronic inflammation associated-oxidative stress occurs in white adipose tissue of the Lantang pig model. In this tissue, up-regulation of pro-inflammatory interleukins (TNF- $\alpha$  and IL-6) coincided with down-regulation of cellular antioxidant enzymes (SOD1 and SOD2) and up-regulation of extracellular SOD.

Cell markers of macrophage and monocytes, TLR4, CD14 and CD11 $\beta$ , were found abundant in subcutaneous adipose tissue of Lantang pig. Consistently, pro-inflammatory factors, MCP1, IL-1 $\beta$ , IL-6 and TNF- $\alpha$ , were also highly expressed in the tissue. These data suggest that chronic inflammation occurred in the adipose tissue of this obese model, which is believed to be a significant physiological characteristics in obese humans and other rodent models (Barbu et al., 2009; de Castro et al., 2011; Lu et al., 2012; Terra et al., 2011). Circulating LPS is demonstrated to be a primary factor for inflammation in obese humans and rodents (Caesar et al., 2012; Clemente-Postigo et al., 2012). In the present study, we also observed a higher plasma LPS level in obese pigs. Enteric LPS in blood is present to all tissues, including subcutaneous, omental and perirenal adipose tissue. However, the inflammatory status was not identical among these adipose tissues as demonstrated by the differential expression of cell markers, CD14 and CD11 $\beta$ , and pro-inflammatory factors, MCP1, IL-1 $\beta$ , IL-6 and TNF- $\alpha$ . In humans and mice, adipose tissues also possess depot-dependent gene expression profile and physiological adaptation (Fried et al., 1998; Kim et al., 2012; Lee et al., 2011). Omental adipose tissue has higher expression of TLR4 and IL-6 protein than subcutaneous adipose tissue in obese subjects (Fried et al., 1998; Kim et al., 2012). Evidence shows that different adipose tissues respond differently to LPS-induced inflammation in non-obese humans (Vatier et al., 2012). It can be inferred that the higher expression of TLR4 accounts for the stronger inflammation induced by LPS, which can further promote the expression of TLR4, particularly in immune cells of adipose tissue. However, the initial factor of the process needs to be determined.

Consistent with obese human and mice (Di Renzo et al., 2010; Furukawa et al., 2004), we found that suppression of cellular antioxidant enzymes, especially SOD1 and SOD2, in subcutaneous adipose tissues associates with activation of MAPK P38 and up-regulation of inflammatory genes. Due to down-regulation of antioxidant enzymes and increased ROS production, adipocytes in obese model tend to have relatively high level of ROS (Furukawa et al., 2004). The increased expression of extracellular superoxide dismutase could be a sign for cellular oxidative stress, which is considered to be a possible compensatory adaptation (Nakao et al., 2000). The intracellular ROS promote the growth and differentiation of adipocytes through cAMP response element-binding protein (CEBP) pathway (Kanda et al., 2011). More importantly, ROS increase the expression of pro-inflammatory factors by activating p38 MAPK (Park et al., 2015; Youn et al., 2016) and NF- $\kappa$ B (Yeop et al., 2010) pro-inflammatory pathways. Antioxidant treatment represses glucose- and palmitate-stimulated ROS generation by inhibiting NF- $\kappa$ B translocation, MCP-1 expression and monocyte chemotaxis in mice (Yeop et al., 2010). Treatment with a SOD mi-

metic reduces omental adiposity and adipose tissue inflammation in high fat fed mice (Pires et al., 2013). It is clear that antioxidant enzymes play critical roles in adipocyte hypertrophy, but the reason why their expressions are selectively suppressed remains to be elucidated. In the present study, we did not observe statistical difference in GPX1 and CAT mRNAs among different adipose tissues, which is inconsistent with results in mice (Furukawa et al., 2004). However, these results further suggest the important role of superoxide dismutase in adipocyte hypertrophy. It also would be interesting to figure out whether the extracellular superoxide dismutase is relevant to monocyte chemotaxis and macrophage infiltration in adipose tissues.

### Conclusion

A new obese model, Lantang pig, is reported in this study to have chronic inflammation associated oxidative stress in adipose tissues, which at least partially, results from the increased presence of circulating LPS and down-regulation of antioxidant enzymes. The porcine model further demonstrates that adipose tissues from different depots show different inflammatory status and antioxidant activities. However, the detailed molecular mechanism underlying the processes of obesity/adiposity development of the present porcine model remains to be further elucidated.

### Conflict of interests

The authors declare no conflicts of interest regarding the publication of this paper.

### References

- Arner P. (1995). Differences in lipolysis between human subcutaneous and omental adipose tissues. *Ann. Med.*, 27: 435–438.
- Barbu A., Hedlund G.P., Lind J., Carlsson C. (2009). Pref-1 and adipokine expression in adipose tissues of GK and Zucker rats. *Mol. Cell. Endocrinol.*, 299: 163–171.
- Bray G.A., Bellanger T. (2006). Epidemiology, trends, and morbidities of obesity and the metabolic syndrome. *Endocrine*, 29: 109–117.
- Caesar R., Reigstad C.S., Backhed H.K., Reinhardt C., Ketonen M., Lunden G.O., Cani P.D., Backhed F. (2012). Gut-derived lipopolysaccharide augments adipose macrophage accumulation but is not essential for impaired glucose or insulin tolerance in mice. *Gut*, 61: 1701–1707.
- Clemente-Postigo M., Queipo-Ortuno M.I., Murri M., Boto-Ordonez M., Perez-Martinez P., Andres-Lacueva C., Cardona F., Tinahones F.J. (2012). Endotoxin increase after fat overload is related to postprandial hypertriglyceridemia in morbidly obese patients. *J. Lipid. Res.*, 53: 973–978.
- de Castro J., Sevillano J., Marciniak J., Rodriguez R., Gonzalez-Martin C., Viana M., Eun-suk O.H., de Mouzon S.H., Herrera E., Ramos M.P. (2011). Implication of low level inflammation in the insulin resistance of adipose tissue at late pregnancy. *Endocrinology*, 152: 4094–4105.
- Deng T., Lyon C.J., Minze L.J., Lin J., Zou J., Liu J.Z., Ren Y., Yin Z., Hamilton D.J., Reardon P.R., Sherman V., Wang H.Y., Phillips K.J., Webb P., Wong S.T., Wang R.F., Hsueh W.A. (2013). Class II major histocompatibility complex plays an essential role in obesity-induced adipose inflammation. *Cell Metab.*, 17: 411–422.
- Di A., Gao X.P., Qian F., Kawamura T., Han J., Hecquet C., Ye R.D., Vogel S.M., Malik A.B. (2012). The redox-sensitive cation channel TRPM2 modulates phagocyte ROS production and inflammation. *Nat. Immunol.*, 13: 29–34.

- Di Renzo L., Galvano F., Orlandi C., Bianchi A., Di Giacomo C., La Fauci L., Acquaviva R., De Lorenzo A. (2010). Oxidative stress in normal-weight obese syndrome. *Obesity* (Silver Spring), 18: 2125–2130.
- Fried S.K., Bunkin D.A., Greenberg A.S. (1998). Omental and subcutaneous adipose tissues of obese subjects release interleukin-6: depot difference and regulation by glucocorticoid. *J. Clin. Endocrinol. Metab.*, 83: 847–850.
- Furukawa S., Fujita T., Shimabukuro M., Iwaki M., Yamada Y., Nakajima Y., Nakayama O., Makishima M., Matsuda M., Shimomura I. (2004). Increased oxidative stress in obesity and its impact on metabolic syndrome. *J. Clin. Invest.*, 114: 1752–1761.
- Harris H.W., Grunfeld C., Feingold K.R., Rapp J.H. (1990). Human very low density lipoproteins and chylomicrons can protect against endotoxin-induced death in mice. *J. Clin. Invest.*, 86: 696–702.
- Hotamisligil G.S., Shargill N.S., Spiegelman B.M. (1993). Adipose expression of tumor necrosis factor- $\alpha$ : direct role in obesity-linked insulin resistance. *Science*, 259: 87–91.
- Kanda Y., Hinata T., Kang S.W., Watanabe Y. (2011). Reactive oxygen species mediate adipocyte differentiation in mesenchymal stem cells. *Life Sci.*, 89: 250–258.
- Kim S., Cho B., Lee H., Choi K., Hwang S.S., Kim D., Kim K., Kwon H. (2011). Distribution of abdominal visceral and subcutaneous adipose tissue and metabolic syndrome in a Korean population. *Diabetes Care*, 34: 504–506.
- Kim S.J., Choi Y., Choi Y.H., Park T. (2012). Obesity activates toll-like receptor-mediated proinflammatory signaling cascades in the adipose tissue of mice. *J. Nutr. Biochem.*, 23: 113–122.
- Lee M.J., Gong D.W., Burkey B.F., Fried S.K. (2011). Pathways regulated by glucocorticoids in omental and subcutaneous human adipose tissues: a microarray study. *Am. J. Physiol. Endocrinol. Metab.*, 300: E571–580.
- Livak K.J., Schmittgen T.D. (2001). Analysis of relative gene expression data using real-time quantitative PCR and the 2<sup>-</sup>( $\Delta\Delta C_T$ ) Method. *Methods*, 25: 402–408.
- Lu C., Zhu W., Shen C.L., Gao W. (2012). Green tea polyphenols reduce body weight in rats by modulating obesity-related genes. *PLoS One*, 7:e38332.
- Motoshima H., Wu X., Sinha M.K., Hardy V.E., Rosato E.L., Barbot D.J., Rosato F.E., Goldstein B.J. (2002). Differential regulation of adiponectin secretion from cultured human omental and subcutaneous adipocytes: effects of insulin and rosiglitazone. *J. Clin. Endocrinol. Metab.*, 87: 5662–5667.
- Nakao C., Ookawara T., Sato Y., Kizaki T., Imazeki N., Matsubara O., Haga S., Suzuki K., Taniguchi N., Ohno H. (2000). Extracellular superoxide dismutase in tissues from obese (ob/ob) mice. *Free Radical Res.*, 33: 229–241.
- Park J., Min J.S., Kim B., Chae U.B., Yun J.W., Choi M.S., Kong I.K., Chang K.T., Lee D.S. (2015). Mitochondrial ROS govern the LPS-induced pro-inflammatory response in microglia cells by regulating MAPK and NF- $\kappa$ B pathways. *Neurosci. Lett.*, 584: 191–196.
- Pires K.M., Ilkun O., Valente M., Boudina S. (2013). Treatment with a SOD mimetic reduces visceral adiposity, adipocyte death and adipose tissue inflammation in high fat fed mice. *Obesity* (Silver Spring), 22: 178–187.
- Spurlock M.E., Gabler N.K. (2008). The development of porcine models of obesity and the metabolic syndrome. *J. Nutr.*, 138: 397–402.
- Terra X., Pallares V., Ardevol A., Blade C., Fernandez-Larrea J., Pujadas G., Salvado J., Arola L., Blay M. (2011). Modulatory effect of grape-seed procyanidins on local and systemic inflammation in diet-induced obesity rats. *J. Nutr. Biochem.*, 22: 380–387.
- Tilg H., Moschen A.R. (2006). Adipocytokines: mediators linking adipose tissue, inflammation and immunity. *Nat. Rev. Immunol.*, 6: 772–783.
- Vatier C., Kadiri S., Muscat A., Chapron C., Capeau J., Antoine B. (2012). Visceral and subcutaneous adipose tissue from lean women respond differently to lipopolysaccharide-induced alteration of inflammation and glyceroneogenesis. *Nutr. Diabetes*, 2:e51.
- Wajchenberg B.L. (2000). Subcutaneous and visceral adipose tissue: their relation to the metabolic syndrome. *Endocr. Rev.*, 21: 697–738.
- Weisberg S.P., McCann D., Desai M., Rosenbaum M., Leibel R.L., Ferrante A.W. Jr. (2003). Obesity is associated with macrophage accumulation in adipose tissue. *J. Clin. Invest.*, 112: 1796–1808.

- Wisse B.E., Kim F., Schwartz M.W. (2007). Physiology. An integrative view of obesity. *Science*, 318: 928–929.
- Yeop Han C., Kargi A.Y., Omer M., Chan C.K., Wabitsch M., O'Brien K.D., Wight T.N., Chait A. (2010). Differential effect of saturated and unsaturated free fatty acids on the generation of monocyte adhesion and chemotactic factors by adipocytes: dissociation of adipocyte hypertrophy from inflammation. *Diabetes*, 59: 386–396.
- Youn G.S., Lee K.W., Choi S.Y., Park J. (2016). Overexpression of HDAC6 induces pro-inflammatory responses by regulating ROS-MAPK-NF- $\kappa$ B/AP-1 signaling pathways in macrophages. *Free Radic. Biol. Med.*, 97: 14–23.

Received: 8 XII 2015

Accepted: 11 VIII 2016

